

Two-photon ionization of He^+ as a nonlinear optical effect in the soft-x-ray region

Kenichi Ishikawa* and Katsumi Midorikawa

Laser Technology Laboratory, RIKEN (The Institute of Physical and Chemical Research), Hirosawa 2-1, Wako-shi, Saitama 351-0198, Japan

(Received 29 November 2001; published 27 March 2002)

We present numerical simulations of two-photon ionization of He^+ by 27th harmonic pulses of a Ti:sapphire laser. This process is chosen as a candidate for the experimental observation of a nonlinear optical effect in the soft-x-ray domain. We solve the time-dependent Schrödinger equation and evaluate the ionization probability as the number of electrons absorbed by the mask function at the outer radial boundary. Our model can address questions concerning possible saturation and quantum interference in ionization at high intensity and ultrashort pulse duration with no ambiguity. According to our results, in spite of saturation of ionization found at intensity higher than 10^{13} W/cm², the ionization probability by a 30 fs harmonic pulse with a peak intensity of $(2-5) \times 10^{13}$ W/cm², attainable with the latest progress in high-order harmonic generation, should be sufficiently high to put the second-order nonlinear optical process in the soft-x-ray region within experimental reach, along with desirable properties such as its nearly quadratic dependence on intensity and approximate linearity in pulse width. Our simulations also show that the variation of the yield with the pulse width of the 27th harmonic is no longer linear for a pulse width shorter than 5 fs, while the dependence on intensity is still quadratic. Our analysis on the ionization of He^+ by a double pulse in such an ultrashort pulse regime shows that the yield is not simply twice as large as that by a single pulse, but exhibits an oscillation of quantum origin with the interval and the phase difference between the two pulses. A simple model of the oscillation is discussed.

DOI: 10.1103/PhysRevA.65.043405

PACS number(s): 32.80.Rm, 32.80.Qk

I. INTRODUCTION

Nonlinear optics [1] is a field in physics with a long history that studies the nonlinear interaction of intense light with matter. Optical phenomena are called nonlinear when the material response to an applied optical field depends on the field strength in a nonlinear fashion. Although theoretical work [2] existed as early as 1931, it was not until the observation of multiphoton transitions between Zeeman sublevels of an atom in the radiofrequency domain [3] that nonlinear optical effects were experimentally demonstrated. Since the discovery of second-harmonic generation [4] and two-photon excitation [5] in 1961, remarkable advances in laser technology have enabled a wide variety of nonlinear optical phenomena [1], including sum- and difference-frequency generation, optical parametric oscillation, intensity-dependent refractive index, multiphoton ionization, and high-order harmonic generation (HHG). Due to considerable progress in the development of x-ray lasers, synchrotron radiation sources, free-electron lasers, and high-order harmonic sources, high-intensity pulses in vacuum and extreme ultraviolet (VUV-XUV) and soft-x-ray regions have now become available.

Among these light sources, the simplicity of HHG is advantageous in that it involves only table-top devices in short pulse duration down to sub-fs [6,7] and in high intensity. Using this type of radiation, two-photon and three-photon ionization [8–10] of rare-gas atoms in VUV and XUV regions was realized. Takahashi *et al.* [11] recently succeeded in the generation of 23rd to 31st harmonic pulses ($\lambda = 25.8$

– 34.8 nm) of a Ti:sapphire laser with a pulse width of 30 fs and an output energy as high as 300 nJ (or 4.5×10^{10} photons) per pulse. When such a soft-x-ray pulse is focused to an area of $10 \mu\text{m}^2$ using a commercially available soft-x-ray mirror, its average intensity may reach 10^{14} W/cm². Now it is time to tackle the problem of inducing nonlinear effects in the soft-x-ray domain. Chen *et al.* [12] proposed second-harmonic generation in the x-ray region using nonlinear optical crystals such as $\beta\text{-BaB}_2\text{O}_4$, LiB_3O_5 , and CsB_3O_5 . However, to our knowledge, its experimental demonstration has not been reported yet. Main obstacles may include high x-ray absorption by these crystals and difficulty in estimating their second-order nonlinear susceptibility.

In the present study, we perform numerical experiments of two-photon ionization of He^+ by the 27th harmonic ($\lambda = 29.6$ nm) of a Ti:sapphire laser as a nonlinear optical effect in the soft-x-ray region. Why He^+ ? Because He^+ is easy to prepare from He, e.g., by means of optical field ionization using an intense laser or single-photon ionization with high-order harmonics. Since the photon energy $\hbar\omega_x = 41.85$ eV is not resonant with the $1s-2p$ transition energy $\hbar\omega_{21} = 40.8$ eV but close to it, high yield (defined as the ratio of the number of produced He^{2+} ions to that of initially present He^+ ions) is expected. Moreover, this simple hydrogenlike system allows us to evaluate yield precisely. In fact, the cross section σ of this process calculated analytically by second-order perturbation theory is 2.9×10^{-52} cm⁴s [13]. This value is only one order of magnitude lower than the two-photon ionization cross section of Xe or Kr by the fifth harmonic (VUV) [10] and that of neutral He by XUV [14]. The number of photons per pulse at the 27th harmonic (up to 8×10^{10}), which is much larger than in the VUV and XUV

*Electronic address: ishiken@postman.riken.go.jp

ranges (up to a few 10^9 [10]), can well compensate for this difference.

Why numerics, if we know the analytical cross section? The two-photon ionization of He^+ is equivalent to that of atomic hydrogen except for a factor stemming from the difference in nuclear charge. The history of analytical calculation of the latter is nearly as long as that of nonlinear optics experiments. A large amount of effort [15] has been devoted to the refinement of the evaluation of transition matrix elements since the first attempt by Zernik [16], and the cross section is tabulated or graphed in the literature [13,17–19]. Strictly speaking, however, these analytical values are valid only at the long-pulse and low-intensity limit. In order for the two-photon ionization of He^+ to be experimentally demonstrated and to be applied to autocorrelation measurements, the variation of the He^{2+} yield with harmonic intensity and pulse width is required to be quadratic and linear, respectively. This relation is not guaranteed *a priori* at high intensity and ultrashort pulse duration considered in the present study. Although experimental investigation exists on multiphoton ionization [20–24] of atomic hydrogen and two-photon ionization from its excited state, corresponding work on two-photon ionization [25] of ground-state hydrogen is lacking. We solve numerically the time-dependent Schrödinger equation (TDSE) for He^+ interacting with an ultrashort intense 27th harmonic pulse, using the alternating direction-implicit method [26]. This type of treatment can deliver an unambiguous answer in the high-intensity and ultrashort pulse regime. Moreover, it can easily handle the temporal variation of intensity.

Our simulations show that the two-photon ionization probability of He^+ is sufficiently high to be experimentally observed, with a yield of 3.3×10^{-4} for the case of a 30 fs pulse whose peak intensity I_{max} is 5×10^{13} W/cm². The dependence of the He^+ yield on I_{max} is still nearly quadratic at this intensity domain, although the ionization rate begins to saturate at $I_{\text{max}} > 10^{13}$ W/cm². On the other hand, the linearity of yield on pulse duration approximately holds for a pulse duration longer than 5 fs, while it breaks down for shorter pulses. Even in the latter case, the yield-intensity relation remains quadratic. Thus, the two-photon ionization probability of He^+ is an attractive candidate for experimental observation of a nonlinear optical effect in the soft-x-ray domain.

Furthermore, we study two-photon ionization by a double pulse in the very short pulse domain (< 5 fs). Our results reveal that quantum interference effects manifest themselves as the dependence of ionization yield on the interval and the phase difference between the two pulses. The resulting oscillation in yield can be explained by a simple model which accounts for direct ionization from the ground state and single-photon ionization from the $2p$ state populated by the first pulse. This region of pulse width, though not suitable for, e.g., autocorrelation experiments, may offer a unique experimental test of quantum mechanics.

The present paper is organized as follows. Section II summarizes the simulation model. In Sec. III, we apply the model to the calculation of the ionization yield of He^+ by a single soft-x-ray pulse, and examine its variation with intensity and pulse duration. In Sec. IV, we study ionization by an

ultrashort double pulse, with focus on the oscillation of the yield with interval and relative phase. The conclusions are given in Sec. V.

II. MODEL

To study the interaction of a He^+ ion initially in the ground state ($1s$) with a soft-x-ray pulse, we solve the time-dependent Schrödinger equation in the length gauge,

$$i \frac{\partial \Phi(\mathbf{r}, t)}{\partial t} = \left[-\frac{1}{2} \nabla^2 - \frac{2}{r} - z E_X(t) \right] \Phi(\mathbf{r}, t), \quad (2.1)$$

where $E_X(t)$ is the electric field of the pulse. Here we have assumed that the field is linearly polarized in the z direction. Equation (2.1) is numerically integrated using the alternating direction-implicit (Peaceman-Rachford) method [26]. The numerical scheme is now well documented [26] and not difficult to implement. To reduce the difference between the discretized and analytical wave function, we scale the Coulomb potential by a few percent at the first grid point [27]. To prevent reflection of the wave function from the grid boundary, after each time step the wave function is multiplied by a $\cos^{1/8}$ mask function [27] that varies from 1 to 0 over a width of $2/9$ of the maximum radius at the outer radial boundary. The ionization yield is evaluated as the decrease of the norm of the wave function on the grid, or equivalently, the number of electrons absorbed by the mask function. In typical calculations, we use a grid with a maximum radius of 125 a.u. and maximum number of partial waves $L_{\text{max}} = 2$. The grid spacing is 0.125 a.u., and the time step is $1/65536$ of an optical cycle t_L of the Ti:sapphire laser light, whose wavelength is 800 nm.

III. TWO-PHOTON IONIZATION PROBABILITY

In this section, we examine the two-photon ionization probability of He^+ by a short, intense 27th-harmonic pulse. As was already mentioned, for applications such as pulse duration measurements by autocorrelation, the ionization probability should be not only sufficiently high but also quadratic in intensity and linear in pulse duration. We consider a single pulse whose electric field is given by

$$E_X(t) = F_X(t) \sin(\omega_X t), \quad (3.1)$$

with F_X being the pulse envelope, chosen to be Gaussian.

A. Dependence on intensity

Figure 1 shows the yield of He^{2+} obtained by a 27th-harmonic pulse with a duration (FWHM) of 30 fs as a function of peak intensity I_{max} . The solid line is the numerical results. The ionization probability is 3.3×10^{-4} at $I_{\text{max}} = 5 \times 10^{13}$ W/cm² and 5.6×10^{-5} at $I_{\text{max}} = 2 \times 10^{13}$ W/cm², which is sufficiently high to be observed experimentally. The dotted line is calculated by the analytical formula $\int_{-\infty}^{\infty} \sigma I(t)^2 dt$, where $I(t)$ denotes the pulse intensity. Below $I_{\text{max}} = 10^{13}$ W/cm² both lines virtually overlap. On the other hand, the numerical result is slightly smaller than the analyti-

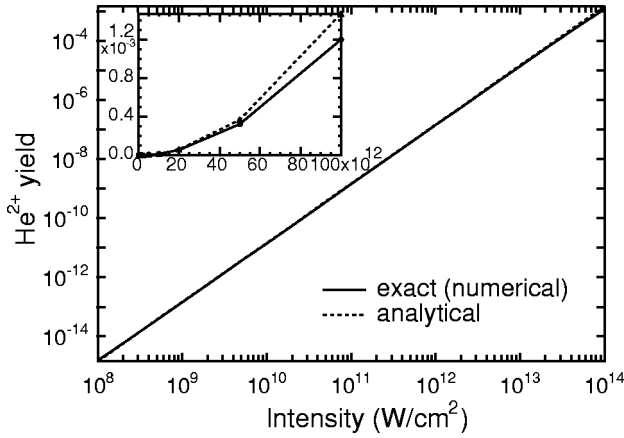


FIG. 1. Yield of He²⁺ vs peak intensity of a Gaussian 27th harmonic pulse with a duration (FWHM) of 30 fs. The solid line denotes numerical results obtained by solving the TDSE, and the dotted line is calculated as $\int_{-\infty}^{\infty} \sigma I(t)^2 dt$. Inset: the same in a linear scale.

cal value at higher intensity. This saturation of the He²⁺ production is more clearly seen in the linear plot in the inset of Fig. 1. It should be noted that this is not due to the decrease of He⁺ [28]. The decrease is as small as 1.2×10^{-3} even at $I_{\max} = 10^{14}$ W/cm². Therefore, this alone cannot explain the difference between the two curves seen in the inset of Fig. 1. Instead, the saturation is mainly due to the quasi-resonant $1s$ - $2p$ transition and the coupling of the $2p$ state with the continuum.

Haberland *et al.* [29] developed a theory with two dressed states coupled to the ionization continuum. Following their theory, the two-photon ionization rate W is given by

$$W = \Gamma_{2p} \left(1 - \frac{d}{2\Omega_R} \right), \quad (3.2)$$

where Γ_{2p} is the energy width of the $2p$ state for ionization to the continuum, $\Omega_R = \sqrt{V^2 + d^2}/4$ is the Rabi frequency, $d = \omega_X - \omega_{21}$ is the detuning, and V is the dipole matrix element between $1s$ and $2p$ states. Since Γ_{2p} and V are proportional to intensity I , the rate W is proportional to I^2 at the low intensity limit and to I at the high intensity limit [25]. Especially at the low intensity limit, W has the following form:

$$W_{\text{low}} = 2\Gamma_{2p} \left(\frac{V}{d} \right)^2, \quad (3.3)$$

and the ratio R of W to W_{low} is given by

$$R = \frac{2}{z} \left(1 - \frac{1}{\sqrt{1+z}} \right), \quad (3.4)$$

where $z = 4V^2/d^2$. $z = I/(3.77 \times 10^{14}$ W/cm²) for the 27th harmonic. In order to compare Eq. (3.4) with a numerical result, we have performed a simulation with a constant intensity of 5×10^{13} W/cm² preceded by a Gaussian ramp which peaks at $t = 133.4$ fs with a FWHM of 90 fs, and we obtained the ionization rate $R_{\text{sim}} = 1.45 \times 10^{10}$ s⁻¹. This

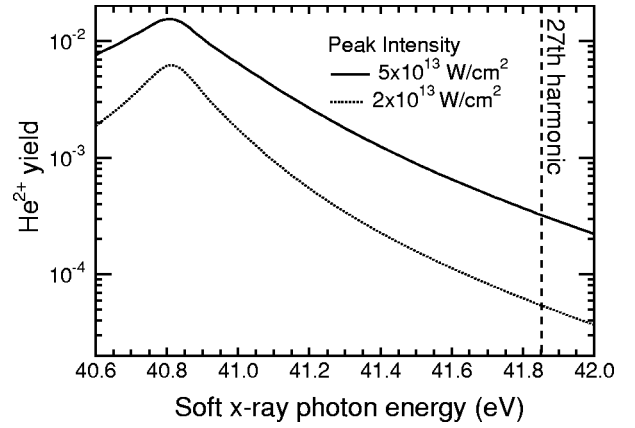


FIG. 2. The yield of He²⁺ as a function of photon energy $\hbar\omega_X$ of a Gaussian pulse with a duration of 30 fs. The solid and dotted lines correspond to peak intensity $I_{\max} = 5 \times 10^{13}$ W/cm² and 2×10^{13} W/cm², respectively.

value is 0.90 of that calculated from the quadratic relation $\sigma I^2 = 1.61 \times 10^{10}$ s⁻¹. This ratio agrees well with the value 0.91 obtained from Eq. (3.4). Thus, the theory by Haberland *et al.* [29], though, strictly speaking, valid only for the long pulse limit, is useful to understand the saturation of the ionization probability as in Fig. 1.

We plot the yield of He²⁺ by a 30 fs Gaussian pulse as a function of photon energy $\hbar\omega_X$ for $I_{\max} = 2 \times 10^{13}$ W/cm² and 5×10^{13} W/cm² in Fig. 2. We also plot their ratio in Fig. 3. As can be seen from these two figures, if the soft-x-ray pulse were closer to the resonance (40.8 eV) than the 27th harmonic is, an approximately quadratic dependence on intensity, one of the desirable properties, would be no longer guaranteed. On the other hand, if it were farther away from the resonance, the ionization probability would be too low. As for the 27th harmonic of a Ti:sapphire laser pulse, the ionization probability is high enough and, at the same time, approximately quadratic in I_{\max} even at I_{\max}

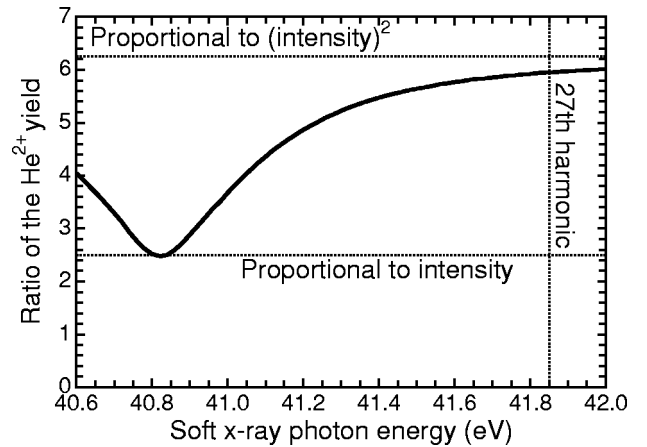


FIG. 3. The ratio of the yield He²⁺ at $I_{\max} = 5 \times 10^{13}$ W/cm² to that at $I_{\max} = 2 \times 10^{13}$ W/cm² as a function of photon energy $\hbar\omega_X$ of a Gaussian pulse with a duration of 30 fs. The upper dotted line indicates the value (6.25) expected for quadratic yield-intensity relation, and the lower (2.5) for linear relation.

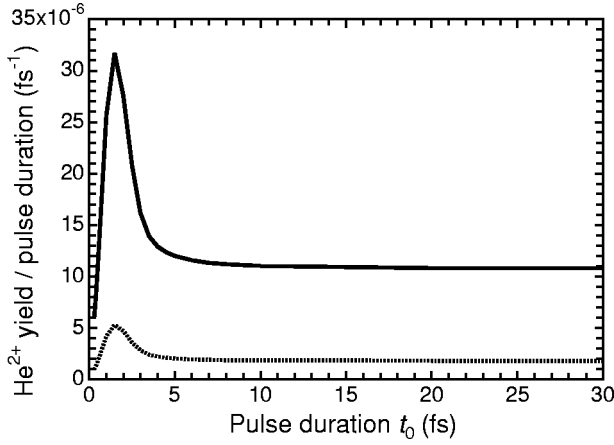


FIG. 4. The He^{2+} yield divided by the pulse duration (FWHM) t_0 of a Gaussian 27th harmonic pulse with a peak intensity of $5 \times 10^{13} \text{ W/cm}^2$ (solid line) and $2 \times 10^{13} \text{ W/cm}^2$ (dotted line) as a function of t_0 . Note that this quantity would be constant for the case of linear dependence of the yield on pulse duration.

$=5 \times 10^{13} \text{ W/cm}^2$ in spite of the saturation. Hence, the 27th harmonic is situated at a very convenient photon energy.

B. Dependence on pulse width

Figure 4 displays the dependence of the He^{2+} yield by a Gaussian 27th harmonic pulse on its pulse duration t_0 (FWHM). The relation is evidently linear at the long pulse limit, but not obvious in an ultrashort pulse regime considered in the present study. In Fig. 4, we can see that the linear relation holds at $t_0 > 5$ fs. In this region, the two-photon ionization of He^+ by the 27th harmonic can be applied for the measurement of pulse duration by autocorrelation. On the other hand, the linearity breaks down for shorter pulses. With decreasing t_0 , the yield-to-pulse-width ratio first increases and then decreases. This can be understood as follows: due to the uncertainty principle, the width of photon energy increases when the pulse duration decreases. The uncertainty in $\hbar\omega_X$ equal to the detuning of 1.05 eV ($=41.85 - 40.8$) corresponds to a pulse duration $t_0 \approx 2$ fs. When the pulse is so short, the $2p$ level is resonantly populated, and, as a result, the ionization probability is augmented. In fact, we have found that the peak position of the photoelectron energy spectrum shifts from 29.3 eV at $t_0 = 6$ fs to 28.8 eV at $t_0 = 2$ fs. Note that $2\hbar\omega_X - U_I = 29.3$ eV and that $\hbar\omega_X + \hbar\omega_{21} - U_I = 28.25$ eV, where U_I denotes the ionization potential of He^+ . When the pulse is shortened further, the bandwidth is so large that most of it is too detuned to induce ionization of He^+ .

In order to examine the dependence of the yield on intensity for such an ultrashort pulse, we plot the ratio of the yield at $I_{\max} = 5 \times 10^{13} \text{ W/cm}^2$ to that at $I_{\max} = 2 \times 10^{13} \text{ W/cm}^2$ as a function of t_0 in Fig. 5. We can see from this figure that even for such a small pulse width for which the linearity is not valid, the ionization probability is still nearly proportional to I_{\max}^2 . For example, in the case of $t_0 = 2$ fs, the ionization probability is 5.5×10^{-5} at $I_{\max} = 5 \times 10^{13} \text{ W/cm}^2$ and 9.4×10^{-6} at $I_{\max} = 2 \times 10^{13} \text{ W/cm}^2$. The ratio 5.9 is close to

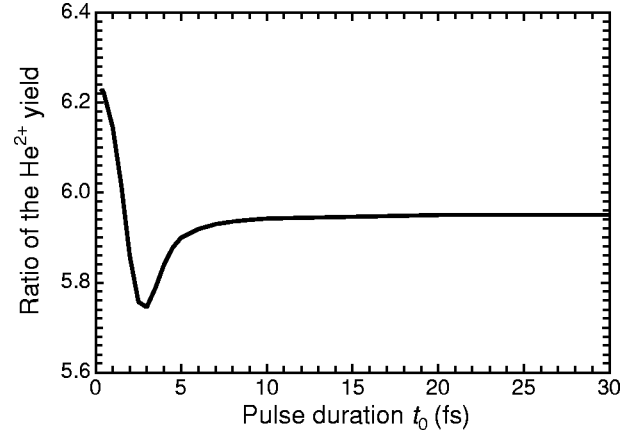


FIG. 5. The ratio of the He^{2+} yield at $I_{\max} = 5 \times 10^{13} \text{ W/cm}^2$ to that at $I_{\max} = 2 \times 10^{13} \text{ W/cm}^2$ as a function of pulse width t_0 (FWHM) of a Gaussian pulse. The value expected for quadratic yield-intensity relation is 6.25.

$(5/2)^2$. Another point to notice is that the yield is nearly perfectly quadratic in I_{\max} for $t_0 < 1$ fs, for which the bandwidth is again so large that most of it is sufficiently detuned for the quadratic relation.

In Fig. 6, we plot the ratio of the ionization probability by a 30 fs pulse to that by a 15 fs pulse as a function of photon energy. The peak intensity is $5 \times 10^{13} \text{ W/cm}^2$. The first autocorrelation experiments in the soft-x-ray range might be performed with such values of pulse width. The yield is approximately linear in pulse duration as long as $\hbar\omega_X$ is not too close to the resonance.

IV. IONIZATION BY DOUBLE PULSE

In this section, we study the two-photon ionization of He^+ by a 27th-harmonic double pulse in detail, especially in the case in which the duration of each pulse is 1 fs. We consider the electric field given by

$$E_X(t) = F_1(t)\sin(\omega_X t + \phi_1) + F_2(t)\sin(\omega_X t + \phi_2), \quad (4.1)$$

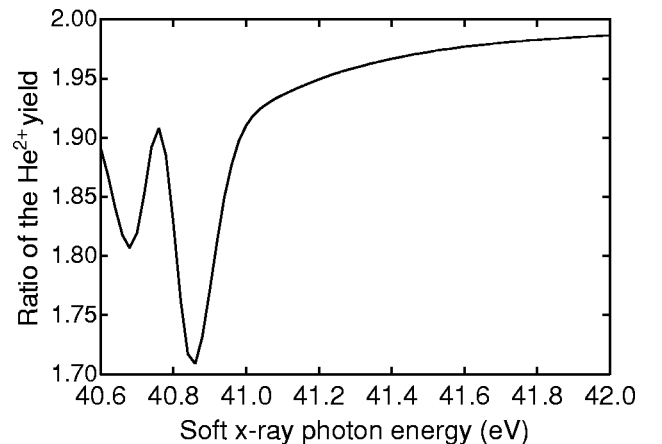


FIG. 6. The ratio of the He^{2+} yield by a Gaussian 27th harmonic pulse at $I_{\max} = 5 \times 10^{13} \text{ W/cm}^2$ with a duration of 30 fs to the yield by a pulse with a duration of 15 fs.

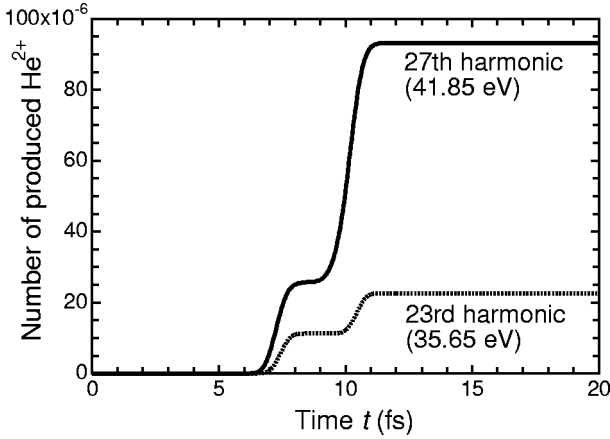


FIG. 7. Temporal evolution of the He²⁺ population by two consecutive 27th harmonic pulses (solid line) and 23rd harmonic pulses (dotted line), respectively. The width (FWHM) of each pulse is 1 fs, the peak intensity is 5×10^{13} W/cm², and the interval between the two pulse peaks is 3 fs.

with $F_{1,2}$ and $\phi_{1,2}$ being the envelope, chosen to be Gaussian, and the phase of each pulse, respectively. The breakdown of the linear dependence of the ionization yield on intensity has a remarkable consequence that the yield of He²⁺ produced by a pulse train is *not* proportional to the number of pulses contained in the train. An example is illustrated in Fig. 7. The solid line is the temporal evolution of the population of He²⁺ produced by two consecutive 1-fs 27th-harmonic pulses, each of which has a peak intensity of 5×10^{13} W/cm² at $t=2t_L$ and $2t_L+3$ fs, respectively, and a phase $\phi_1=\phi_2=0$. The production of He²⁺ by the second pulse is much larger than that by the first pulse. Such a situation is not suitable for the pulse width measurement by autocorrelation. When the pulse is as short as 1 fs, the autocorrelation experiments are possible only for more detuned pulses such as the 23rd harmonic ($\hbar\omega_X=35.65$ eV), the result for which is plotted as a dotted line in Fig. 7.

Let us now, however, look at this situation from a completely different point of view. The breakdown of linearity is a quantum effect which cannot be observed using longer pulses. The progress of the pulse compression technique may enable the observation of such quantum effects. It is, therefore, important to study how the final yield of He²⁺ by double pulse irradiation depends on the interval between the two pulses and on their relative phase.

Figure 8 shows the He²⁺ yield by a 1-fs 27th-harmonic double pulse as a function of ϕ_2 . Each pulse has a peak intensity of 5×10^{13} W/cm² at $t=2t_L$ and $2t_L+4.148$ fs, respectively. The solid line is for $\phi_1=0$ and the dashed line is for $\phi_1=\pi/2$. We also plot the yield by a single pulse as a function of ϕ_1 as a dotted line. In the last case, the yield is seen to be independent of ϕ_1 , since the pulse is still much longer than the optical period (0.0988 fs) of the harmonic. On the other hand, in the case of double pulses, the final yield of He²⁺ is an oscillating function of $\Delta\phi=\phi_2-\phi_1$. After the first pulse has passed, He⁺ is in a superposition of $1s$ and $2p$ states (the $2p$ population is 7.2×10^{-2}). Such a system has a dipole moment oscillating with a frequency

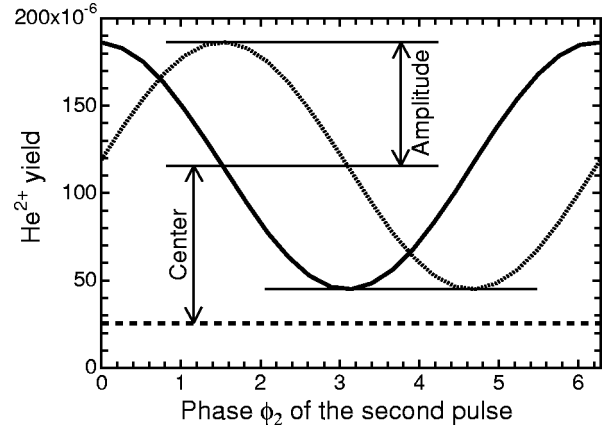


FIG. 8. He²⁺ yield by a 27th harmonic double pulse whose electric field is of the form Eq. (4.1) as a function of ϕ_2 . Each pulse with a duration of 1 fs has a peak intensity of 5×10^{13} W/cm² at $t=2t_L$ and $2t_L+4.148$ fs, respectively. Solid curve: $\phi_1=0$. Dotted curve: $\phi_1=\pi/2$. Dashed line: He²⁺ yield by a single pulse as a function of ϕ_1 .

corresponding to the energy difference $\hbar\omega_{21}=3/2$ a.u. between $2p$ and $1s$. Its period T_d is 0.1013 fs. The relation between the phase of the oscillating dipole moment and that of the second soft-x-ray pulse causes an oscillation in the He²⁺ yield as seen in Fig. 8.

In order to confirm this further, we have performed simulations by varying the interval Δt between the two pulse peaks. ϕ_1 is fixed to zero and $\phi_2=-\omega_X\Delta t$. Note that by such a choice of ϕ_1 and ϕ_2 , not only the intensity of the second pulse but also the electric field itself is shifted by Δt with respect to the first pulse. This is a situation realized in usual autocorrelation experiments. The simulation result is plotted in Fig. 9. It is clear that the yield oscillates with the same period as the dipole moment (T_d).

Let us now investigate how the center and the amplitude of the oscillation as in Figs. 8 and 9 depend on pulse inten-

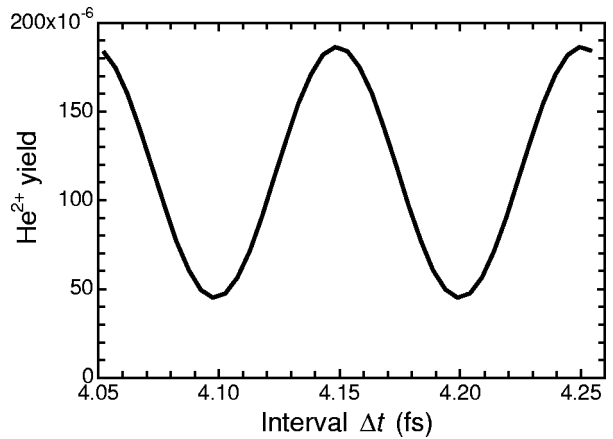


FIG. 9. He²⁺ yield by a 27th harmonic double pulse as a function of the interval Δt between the two pulse peaks. Each pulse has a Gaussian temporal profile with a duration of 1 fs and a peak intensity of 5×10^{13} W/cm². The first pulse peaks at $t=2t_L$. $\phi_1=0$ and $\phi_2=-\omega_X\Delta t$.

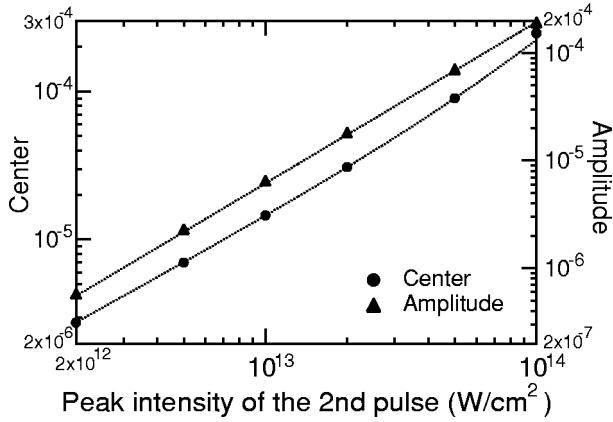


FIG. 10. The center (circle, left axis) and the amplitude (triangle, right axis) of the oscillation of the number of He^{2+} produced by the second pulse as a function of its peak intensity. Each pulse has a width of 1 fs, and the peak intensity of the first pulse is $5 \times 10^{13} \text{ W/cm}^2$. Dotted lines are the fitting curves obtained using Eq. (4.3).

sity. We have performed simulations by varying the peak intensity of the second pulse while fixing that of the first pulse to $5 \times 10^{13} \text{ W/cm}^2$, and we obtained the center and the amplitude, as defined in Fig. 8, of the oscillation of the number of He^{2+} produced by the second pulse. Their dependence on the peak intensity of the second pulse is shown in Fig. 10. The production of He^{2+} by the second pulse proceeds in two ways: one-photon ionization from $2p$ and two-photon ionization from $1s$. By taking their interference into account, the transition amplitude of the entire process has the following form:

$$\sqrt{(\alpha_0 I_1)(\alpha_1 I_2)} + \sqrt{(1 - \alpha_0 I_1)(\alpha_2 I_2^2)} e^{i(\Delta\phi + \phi_0)}, \quad (4.2)$$

where $I_{1,2}$ is the peak intensity of the first and the second pulse, respectively. $\alpha_0 I_1$ describes the excitation of the $2p$ level by the first pulse, $\alpha_1 I_2$ the ionization from $2p$ to the continuum, and $\alpha_2 I_2^2$ the two-photon ionization from $1s$. Then we can write the number of He^{2+} produced by the second pulse as

$$aI_2 + bI_2^2 + cI_2^{3/2} \cos(\Delta\phi + \phi_0), \quad (4.3)$$

where

$$a = \alpha_0 \alpha_1 I_1, \quad (4.4)$$

$$b = (1 - \alpha_0 I_1) \alpha_2 \approx \alpha_2, \quad (4.5)$$

$$c = 2\sqrt{ab}. \quad (4.6)$$

The simulation result in Fig. 10 is very well fitted by a function of the form in Eq. (4.3) as is shown by dotted curves, though a small discrepancy is found for the highest value of I_2 . The coefficients a , b , and c obtained by the fitting are listed in Table I along with their values for the case of I_1

TABLE I. The parameters a , b , and c obtained by fitting the numerically obtained values of center and amplitude of the oscillation of the He^{2+} yield by the second pulse with Eq. (4.3). The intensity is in W/cm^2 . c_{th} is the value of c calculated from a and b with Eq. (4.6). The numbers in brackets indicate powers of 10.

Intensity	a	b	c	c_{th}
5[13]	1.37[-18]	8.67[-33]	2.00[-25]	2.18[-25]
2[13]	5.67[-19]	9.77[-33]	1.35[-25]	1.49[-25]

$= 2 \times 10^{13} \text{ W/cm}^2$. From Table I, a is proportional to I_1 while b is approximately constant as is expected from Eqs. (4.4) and (4.5), respectively. The relation Eq. (4.6) is also roughly satisfied. Hence, the oscillation of the He^{2+} yield can be explained essentially by the simple phenomenological model discussed above.

V. CONCLUSIONS

Using numerical simulations, we have examined the suitability of two-photon ionization of He^+ by a 27th harmonic pulse of a Ti:sapphire laser as a system for the experimental observation of a nonlinear optical effect in the soft-x-ray region. We have considered the pulse parameters accessible with a state-of-the-art high-order harmonic generation technique, namely, intensity up to $5 \times 10^{13} \text{ W/cm}^2$ and pulse width as short as 1–30 fs. Our simulation results have revealed that such an ultrashort intense harmonic pulse should be sufficient to render realistic the observation of the second-order nonlinear optical process. Although the saturation effect reduces the ionization probability by about 10% at $I_{\text{max}} = 5 \times 10^{13} \text{ W/cm}^2$, the variation of the He^{2+} yield with intensity is nearly quadratic even in this high-intensity region. Moreover, the ionization is approximately proportional to the pulse width at $t_0 > 5$ fs. These properties are desirable for the experimental demonstration of the nonlinear effect.

Our analysis of two-photon ionization by a harmonic double pulse with a duration of 1 fs has shown that the interference between the direct two-photon process from the ground state and the single-photon process from the $2p$ state populated by the first pulse induces oscillation in the He^{2+} yield with the interval and the phase difference between the two pulses. The excitation to the $2p$ level is possible due to the large bandwidth associated with the ultrashort pulse width. The oscillation period is precisely predictable from the $1s$ - $2p$ transition energy. The detection of such an oscillation may serve as a unique test of quantum mechanics.

ACKNOWLEDGMENTS

We would like to thank I. Koprnikov, H. Okamura, Y. Nabekawa, and E. Takahashi for fruitful discussions, especially on experimental feasibility. This work was supported by the Special Postdoctoral Researchers Program and the President's Special Research Grant of RIKEN.

- [1] R.W. Boyd, *Nonlinear Optics* (Academic, Boston, 1992).
- [2] M. Göppert-Mayer, *Ann. Phys. (Leipzig)* **9**, 273 (1931).
- [3] J.M. Winter, *Ann. Phys. (Paris)* **4**, 745 (1959).
- [4] P.A. Franken, A.E. Hill, C.W. Peters, and G. Weinreich, *Phys. Rev. Lett.* **7**, 118 (1961).
- [5] W. Kaiser and C.G.B. Garrett, *Phys. Rev. Lett.* **7**, 229 (1961).
- [6] P.M. Paul, E.S. Toma, P. Breger, G. Mullot, F. Augé, Ph. Balcou, H.G. Muller, and P. Agostini, *Science* **292**, 1689 (2001).
- [7] M. Hentschel, R. Kienberger, Ch. Spielmann, G.A. Reider, N. Milosevic, T. Brabec, P. Corkum, U. Heinzmann, M. Drescher, and F. Krausz, *Nature (London)* **414**, 509 (2001).
- [8] Y. Kobayashi, T. Sekikawa, Y. Nabekawa, and S. Watanabe, *Opt. Lett.* **23**, 64 (1998).
- [9] Y. Kobayashi, T. Ohno, T. Sekikawa, Y. Nabekawa, and S. Watanabe, *Appl. Phys. B: Lasers Opt.* **70**, 389 (2000).
- [10] D. Descamps, L. Roos, C. Delfin, A. L'Huillier, and C.-G. Wahlström, *Phys. Rev. A* **64**, 031404 (2001).
- [11] E. Takahashi, Y. Nabekawa, T. Otuka, M. Obara, and K. Midorikawa (unpublished).
- [12] T.-J. Chen, R.N. Zitter, and R. Tao, *Phys. Rev. A* **51**, 706 (1995).
- [13] F.T. Chan and C.L. Tang, *Phys. Rev.* **185**, 42 (1969).
- [14] A. Saenz and P. Lambropoulos, *J. Phys. B* **32**, 5629 (1999).
- [15] A.P. Jayadevan and R.B. Thayyullathil, *J. Phys. B* **34**, 699 (2001), and references therein.
- [16] W. Zernik, *Phys. Rev.* **135**, A51 (1964).
- [17] H.B. Bebb and A. Gold, *Phys. Rev.* **143**, 1 (1966).
- [18] Y. Gontier and M. Trahin, *Phys. Rev.* **172**, 83 (1968).
- [19] G. Laplanche, A. Durrieu, Y. Flank, M. Jaouen, and A. Rachman, *J. Phys. B* **9**, 1263 (1976).
- [20] M. LuVan, G. Mainfray, C. Manus, and I. Tugov, *Phys. Rev. A* **7**, 91 (1973).
- [21] D.E. Kelleher, M. Ligare, and L.R. Brewer, *Phys. Rev. A* **31**, 2747 (1985).
- [22] H.G. Muller, H.B. van Linden van den Heuvell, and M.J. van der Wiel, *Phys. Rev. A* **34**, 236 (1986).
- [23] H. Rottke, B. Wolff, M. Brickwedde, D. Feldmann, and K.H. Welge, *Phys. Rev. Lett.* **64**, 404 (1990).
- [24] R.S.D. Sihombing, M. Katsuragawa, G.Z. Zhang, and K. Hakuta, *Phys. Rev. A* **54**, 1551 (1996).
- [25] P. Antoine, N.-E. Essarroukh, J. Jureta, X. Urbain, and F. Brouillard, *J. Phys. B* **29**, 5367 (1996).
- [26] K.C. Kulander, K.J. Schafer, and J.L. Krause, in *Atoms in Intense Laser Fields*, edited by M. Gavrilu (Academic, New York, 1992), pp. 247–300.
- [27] J.L. Krause, K.J. Schafer, and K.C. Kulander, *Phys. Rev. A* **45**, 4998 (1992).
- [28] M.V. Ammosov, N.B. Delone, M.Y. Ivanov, and A.V. Masalov, *Adv. At., Mol., Opt. Phys.* **29**, 33 (1991).
- [29] H. Haberland, M. Oschwald, and J.T. Broad, *J. Phys. B* **20**, 3367 (1987).